Supporting Information for:

Controlled Hysteresis of Conductance in Molecular Tunneling Junctions

Junwoo Park,[1,2,⊥] Mohamad S. Kodaimati,[1,⊥] Lee Belding,[1] Samuel E. Root,[1] George C. Schatz,[3] and George M. Whitesides[1,*]

[1] Department of Chemistry and Chemical Biology, Harvard University, 12 Oxford Street, Cambridge, Massachusetts 02138, United States

[2] Department of Chemistry, Sogang University, Mapo-gu, Seoul 04107, Republic of Korea

[3] Department of Chemistry, Northwestern University, 2145 Sheridan Rd., Evanston, IL 60208-3113, United States.

⊥ J.P. and M.S.K. contributed equally to this work.

(*) Author to whom correspondence should be addressed: gwhitesides@gmwgroup.harvard.edu

Materials and Methods

We followed previously reported procedures for the preparation of materials and experimental methods,[1] and included a description of the experiments that were conducted in the same way.

Materials

All reagents were used as supplied unless otherwise specified. All organic solvents in analytical grade (99%) were purchased from Sigma-Aldrich. The 1-octadecanethiol was purchased from Sigma-Aldrich (>98% purity). High purity eutectic gallium-indium (EGaIn; 99.99%) was obtained from Sigma-Aldrich and used as supplied.

Choice of Electrodes

Template-stripped Au surfaces (Au^{TS}) served as bottom electrodes.[2] Molecules (*i.e.*, $S(CH_2)_{11}BIPY$) align on the Au surface, and form SAMs.[3] The surface roughness and defects can increase the variance in the measured tunneling current or result in more frequent electrical shorts. We, thus, used ultraflat Au^{TS} to minimize the defects of the surface, and the root-mean-square roughness for Au^{TS} surface was 5.1 ± 0.4 nm (over an area of 25 μm^2).[2] GaO_x/EGaIn served as a top electrode which enables non-damaging soft contact, as well as the simple and rapid measurement of current density.[4] A native oxide layer (a few atomic layers thick) of EGaIn results in the non-Newtonian character of the GaO_x/EGaIn liquid metal: GaO_x/EGaIn maintains a conical shape (which is not a minimum in the surface energy) and behaves as a solid that yields at a critical stress. These features (i) enables measurements under ambient conditions, and (ii) prevents the SAMs from being damaged by the contact, resulting in high yield (70-90%).[4]

Preparation of BIPY-MCl_2 Junctions

Our synthesis of the BIPY-containing SAMs, which consists of an insulating alkyl chain terminated by a BIPY moiety, followed a procedure from the literature.[5] SAMs of $S(CH_2)_{11}$BIPY were formed by immersion of a smooth template-stripped (TS) gold surface (Au^{TS}) in 1.0 mM ethanolic solutions of thiol-terminated molecules for 18 hours under a nitrogen atmosphere. The BIPY moieties were complexed with metal (II) chlorides by incubating the SAM within a 10-mM solution of metal (II) chloride in ethanol to form Au^{TS}-$S(CH_2)_{11}$BIPY-MCl_2 junctions, also under a nitrogen atmosphere for 18 hours. After each immersion, we gently rinsed the samples with ethanol for one minute (~1 ml/min) to remove residue on the surface and dried the samples under a slow flow of nitrogen gas. In BIPY-MCl_2 junctions, metal(II) complexed with SAMs of alkanethiolates terminated by 2,2'-bipyridine (Au^{TS}-$S(CH_2)_{11}$BIPY-M) with 1:1 stoichiometry. To minimize uncertainties, (i) all the BIPY-MCl_2 junctions are complexed with metals which have the same principal quantum number, (ii) the oxidation state of metals in as-fabricated BIPY-MCl_2 junctions is +2, and (iii) the counterions are all chloride ions. BIPY-$CoCl_2$ and BIPY-$CuCl_2$ complex probably has a structure of distorted tetrahedral.[6–8]

Characterization: J−V Measurements

We performed the measurements within one hour of the samples being prepared. After placing the samples (Au^{TS}-$S(CH_2)_{11}$BIPY-M(II)Cl_2^-) on the anti-vibration table, we connected a grounded Au surface to the negative port of a source meter (6430 Sub-Femtoamp Remote SourceMeter, Keithley). A 10-μL Hamilton syringe containing eutectic indium-gallium (EGaIn, 75.5 % Ga 24.5 %, and superficial layer of GaO_x) alloy, serving as a top electrode, was

controlled by a micromanipulator, and was connected to the port of the source meter. We formed an EGaIn tip of conical shape by extruding an EGaIn drop from the syringe on a clean Si wafer,[4,9] and bringing the EGaIn tip gently into contact with the samples (contact area ~ 900 μm^2). A voltage was subsequently applied to the EGaIn tip (positive voltage corresponds to EGaIn oxidizing and negative voltage corresponds to EGaIn reducing), and current flowing across the junctions was measured (one trace from 0 V to +1.0 V to −1.0 V to 0 V).

XPS Measurements

We used XPS to characterize Au^{TS}-$S(CH_2)_{11}$BIPY-M(II)Cl_2 with instruments located in the Center for Nanoscale System at Harvard University. The energy of the incident X-ray beam used by the Thermo Scientific K-Alpha XPS system is at 1486.6 eV. We recorded high-resolution XPS spectra of S 2p, C 1s, N 1s, Au 4f, and Metal 2p. We used a least-square algorithm to fit the peak with a pseudo-Voigt function (a linear combination of Lorentzian (30 %) and Gaussian (70 %) functions)[10] using the XPSpeak software.[11] The sloping background was modeled using a Shirley plus linear background correction.[12] The pseudo-Voight functions is used because it is well-known that instrumental factors (*e.g.*, resolution of the analyzer or monochromator) and experimental factors (*e.g.*, surface roughness of the samples, vibrational effect, and polarization effects) manifest as Gaussian broadening of the ideally Lorentzian signals of photoelectrons.[13]

We calculated elemental ratios from the ratios of integrated area of XPS spectrum, and expect the the observation of uncorrected atomic ratios of nitrogen to sulfur being higher than two (Table S1) is due to the probability of photoelectrons emitted from the sulfur atom reaching the detector being lower than that of nitrogen, due to the density and thickness of the SAMs. We

corrected the atomic ratios of nitrogen to sulfur with thickness of SAMs based on the exponential attenuation of signal intensity by the thickness of SAMs.[14,15]

Preparation of Junctions for Temperature-Dependence Experiments

We follow the method reported in the literature for the fabrication of molecular junctions used in temperature-dependence experiments.[16] The EGaIn tip was brought into contact gently with the samples (Au^{TS}-$S(CH_2)_{11}$BIPY-M(II)Cl_2), with the contact area of ~ 900 μm^2. A drop of photocurable polymer (Norland Optical Adhesive 61, Norland Products) was placed on the sample near the EGaIn electrode to surround the Au^{TS}-$S(CH_2)_{11}$BIPY-M(II)Cl_2//Ga_2O_3/EGaIn by the photocurable polymer. As we exposed the junctions to UV light using a hand-held lamp for a few seconds (~5 s), the EGaIn electrode in conical shape was encapsulated with the cured polymer. Then, we gently lifted the syringe containing EGaIn to form encapsulated BIPY-MCl_2 junctions.

Density-Functional Theory Calculations.

Quantum chemical calculations were calculated at the DFT level using Nwchem 6.6[17] software with the B3LYP hybrid functional. All calculations were performed using an open-shell configuration where the spin was specified. We performed initial calculations and optimization of the molecular geometries using the 6-311++** basis sets for H, C, N, and Cl atoms and lanl2dz effective core potentials (ecp) for the S, Co, and Cu atoms. After the geometry optimization, we performed DFT calculations with the aug-cc-pvdz basis sets for H, C, N, and Cl atoms and lanl2dz effective core potentials (ecp) for the S, Co, and Cu atoms. We visualized the DFT orbitals using Avogadro.[18]

Raman Spectroscopy

To determine the effect of the applied potential on the molecular conformations of the BIPY-Co(II)Cl_2 junctions, we employed confocal Raman spectroscopy to measure the Raman spectrum of the SAMs. Raman measurements were carried out using a Horiba LabRam HR Evolution confocal Raman microscopy with 633 nm excitation (~10 mW). The Raman measurements were averaged over 25 spots on the SAMs with 5 measurements collected each for 300 s with a 150 um pinhole and 600 gr/mm grating. The spectra were corrected for stray cosmic rays, and the spectrograph was calibrated to a Si wafer (peak at 520.7 cm^-) prior to each measurement. All spectra shown are subtracted for a bare Au sample. We performed Raman measurements by imaging through the Au layer on samples deposited on 30 nm template stripped-Au and encapsulated using optical adhesive. A voltage was applied to the SAM through the EGaIn electrode using a Keithley 2400.

Table S1. Elemental Ratios in the Au^{TS}-$S(CH_2)_{11}$BIPY-M(II)Cl_2 junctions (M = Cr, Mn, Fe, Co, Ni, and Cu) characterized by X-ray photoelectron spectroscopy (XPS). Experiments were replicated a total of ten times, and uncertainty values represent the standard deviation.

BIPY-MCl_2 junctions	Cr	Mn	Fe	Co	Ni	Cu
Sulfur : Nitrogen	1 : 2.85 ± 0.04	1 : 2.90 ± 0.06	1 : 2.87 ± 0.08	1 : 2.74 ± 0.05	1 : 2.73 ± 0.08	1 : 2.72 ± 0.08
Metal : Nitrogen	1 : 2.20 ± 0.19	1 : 1.82 ± 0.18	1 : 1.86 ± 0.13	1 : 1.81 ± 0.14	1 : 2.24 ± 0.13	1 : 1.88 ± 0.12
Metal : Chloride	1 : 1.14 ± 0.11	1 : 1.34 ± 0.12	1 : 1.55 ± 0.09	1 : 1.85 ± 0.06	1 : 1.16 ± 0.07	1 : 1.72 ± 0.16

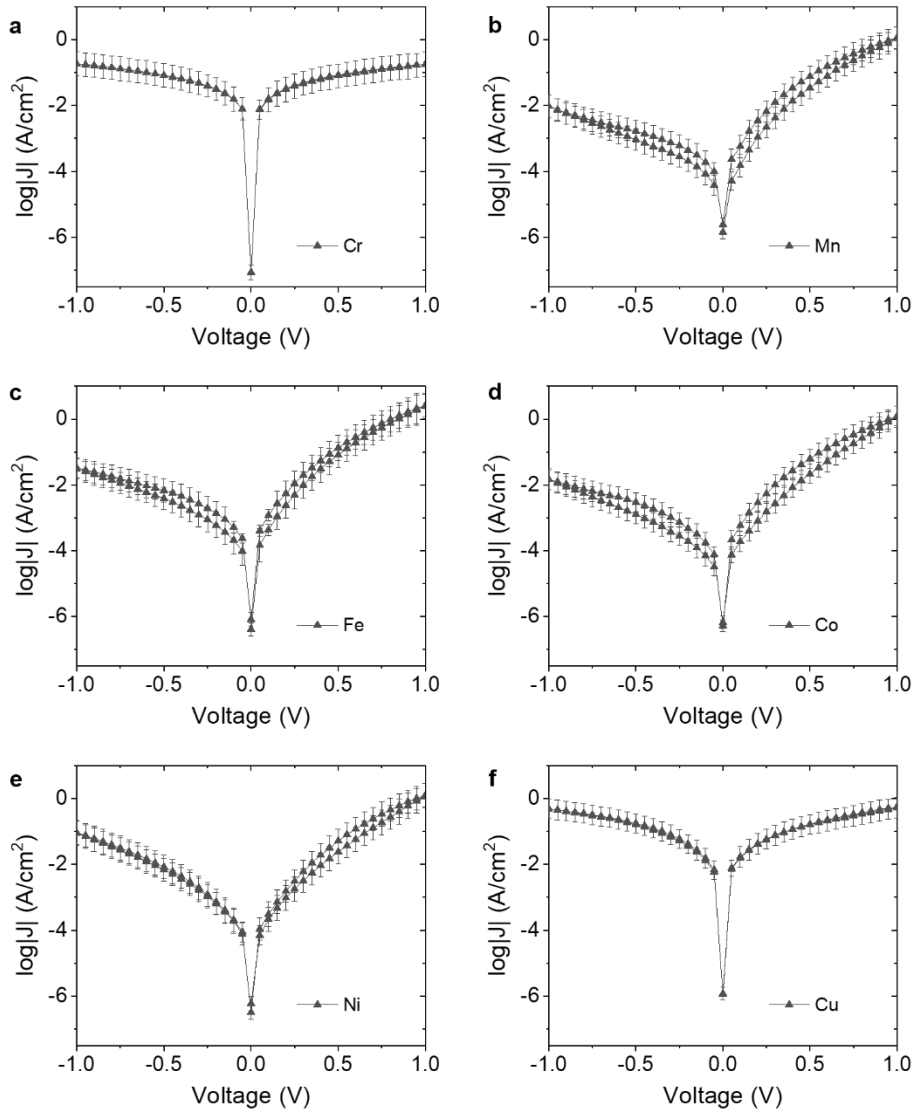

Fig. S1. Averaged J(V) traces of (a-f) Au^{TS}-$S(CH_2)_{11}BIPY$-MCl_2//GaO_x/EGaIn junctions (M = (a) Cr, (b) Mn, (c) Fe, (d) Co, (e) Ni, and (f) Cu).

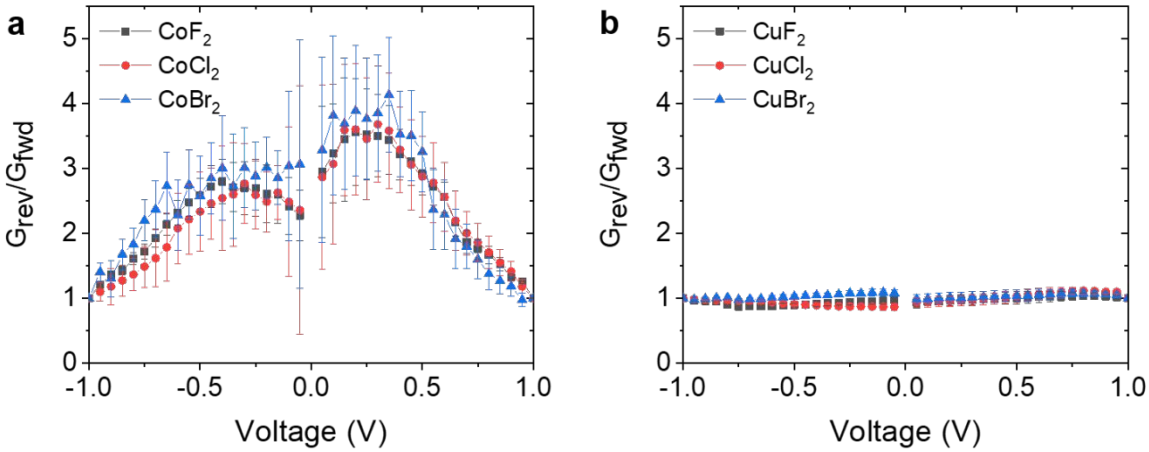

Fig. S2. The ratio of conductance for the forward and reverse scan in (a) BIPY-Co and (b) BIPY-Cu junctions which complexed with halide anions. The error bars represent the standard deviation.

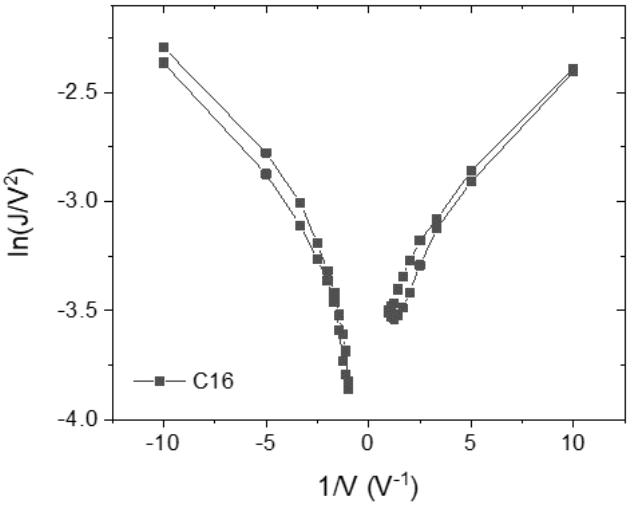

Figure S3. Fowler-Nordheim (FN) plots for junctions composed of alkanethiolates SAMs: Au^{TS}-$S(CH_2)_{15}CH_3$//GaO_x/EGaIn. Voltage window is -1.0 V to +1.0 V

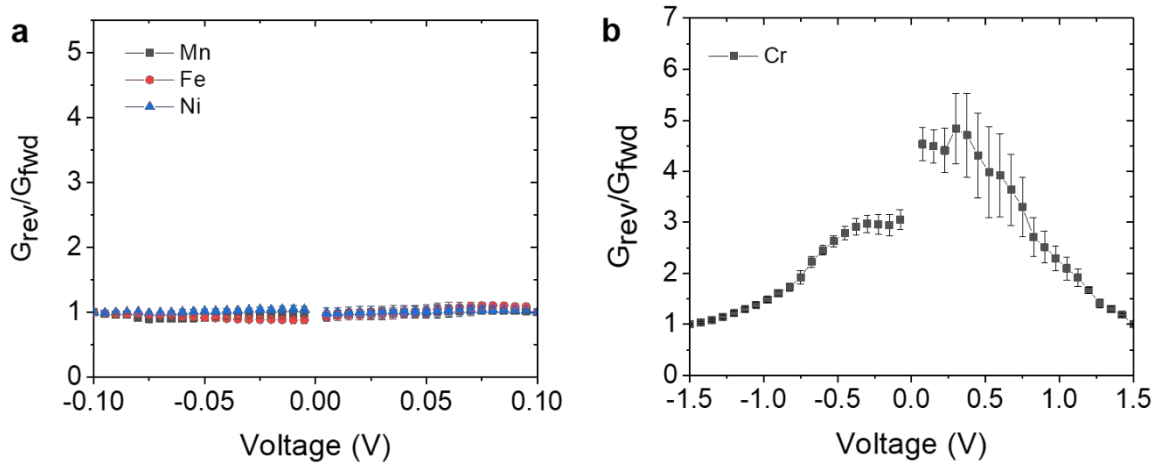

Fig. S4. The ratio of conductance for forward and reverse scan in BIPY-MCl_2 junctions complexed with (a) BIPY-Mn, Fe, Ni (a voltage window of ±0.1 V) and (b) BIPY-$CrCl_2$ junctions (a voltage window of ±1.5 V).

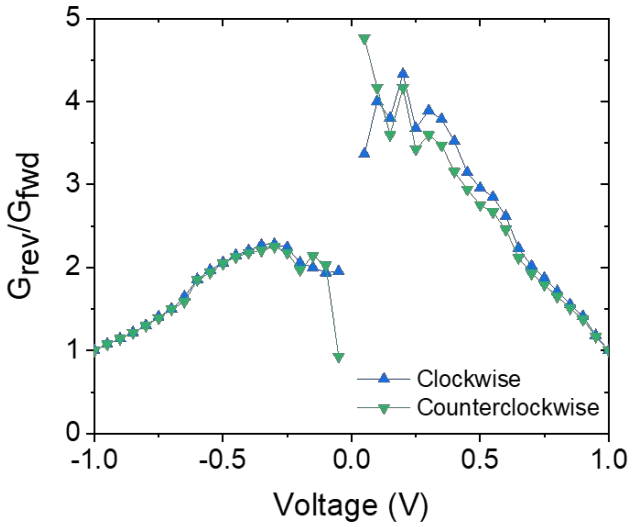

Fig. S5. The ratio of conductance for forward and reverse scan in BIPY-$CoCl_2$ junctions with the opposite direction of voltage sweep.

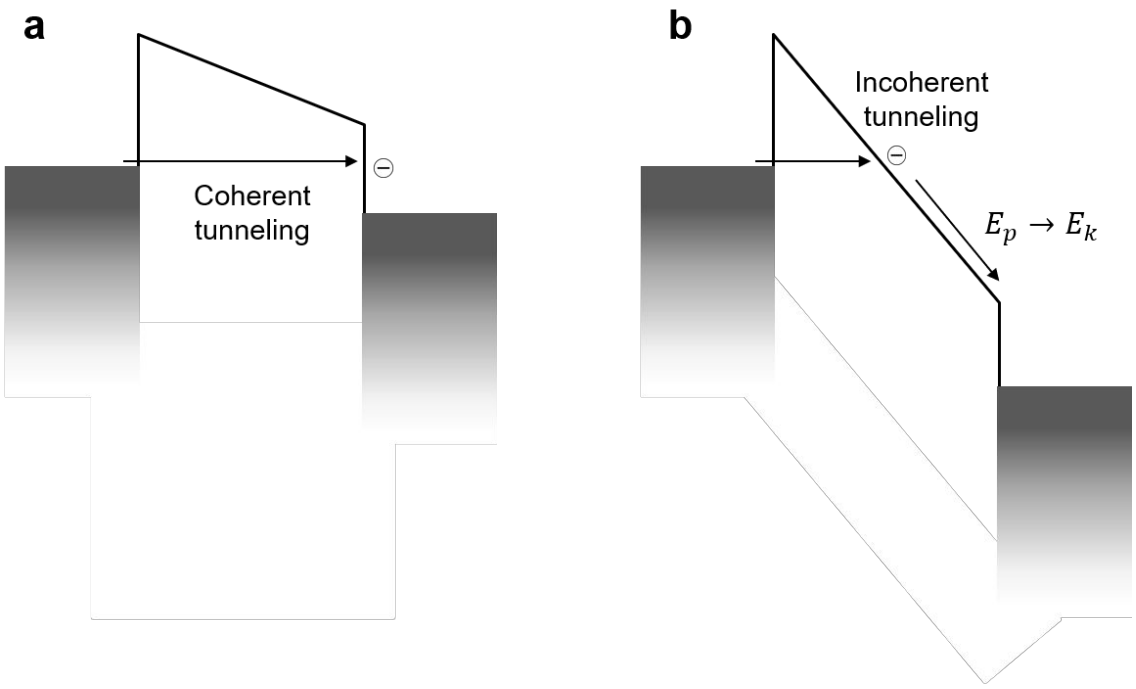

Fig. S6. Energy level diagrams (defined by LUMO of alkyl chain) in (a) direct and (b) FN tunneling conditions.

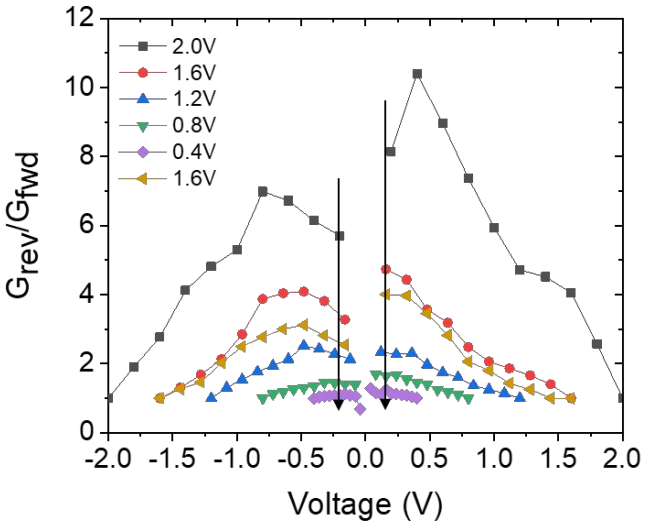

Fig. S7. The magnitude of hysteresis (G_{rev}/G_{fwd}) in BIPY-$CoCl_2$ junctions with the change in voltage window.

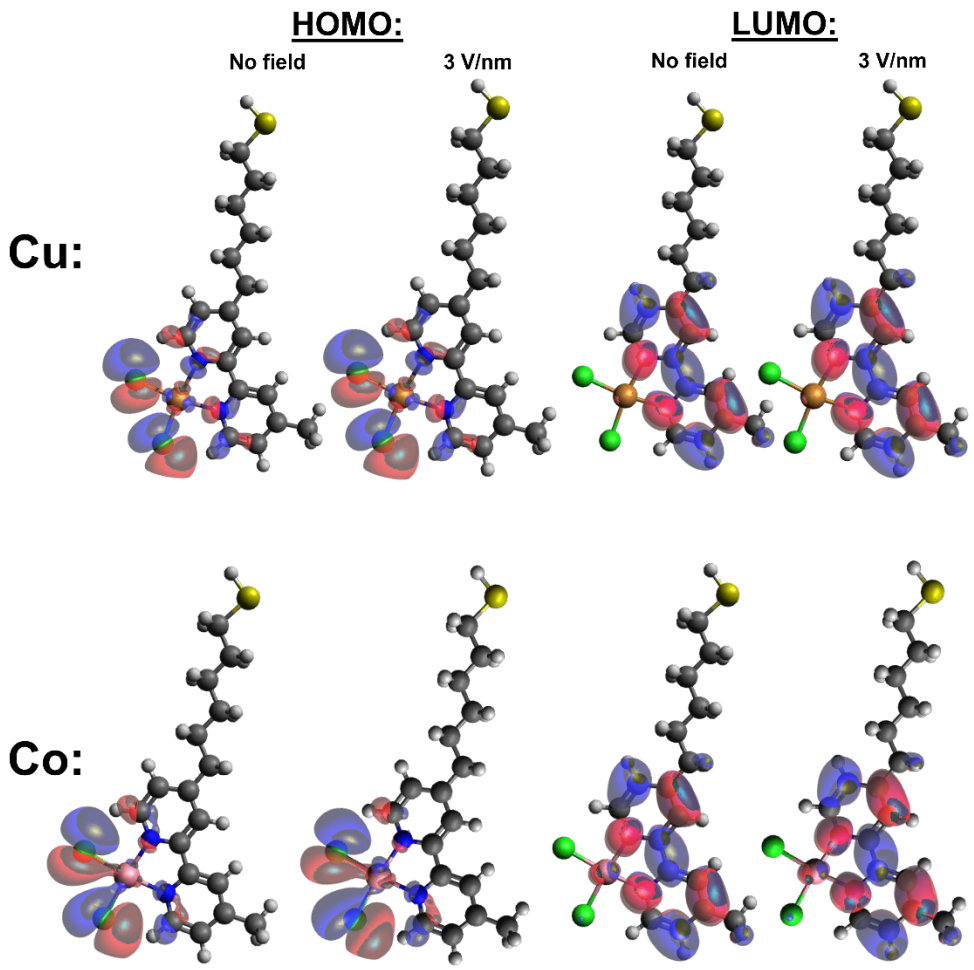

Fig. S8. HOMO and LUMO orbitals generated by DFT of BIPY-$CuCl_2$ and BIPY-$CoCl_2$ with no applied field and a field of 3 V/nm.

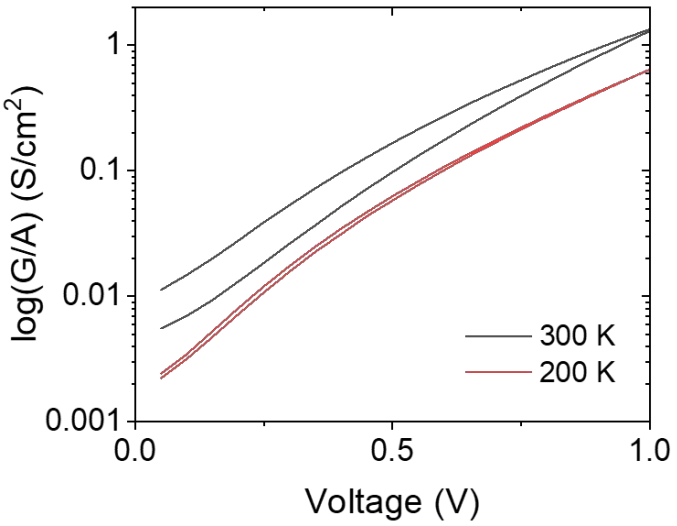

Fig. S9. Averaged plots of conductance per unit contact area in log-scale *versus* applied voltage traces measured in Co junctions measured at 300 K and 200 K.

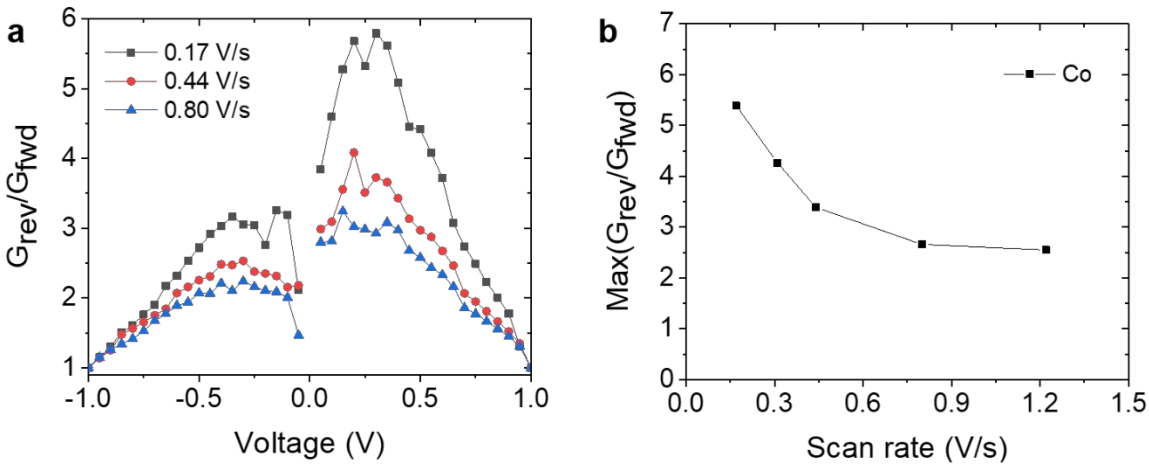

Fig. S10. The ratio of conductance for forward and reverse scan in BIPY-$CoCl_2$ junctions with changing scan rate.

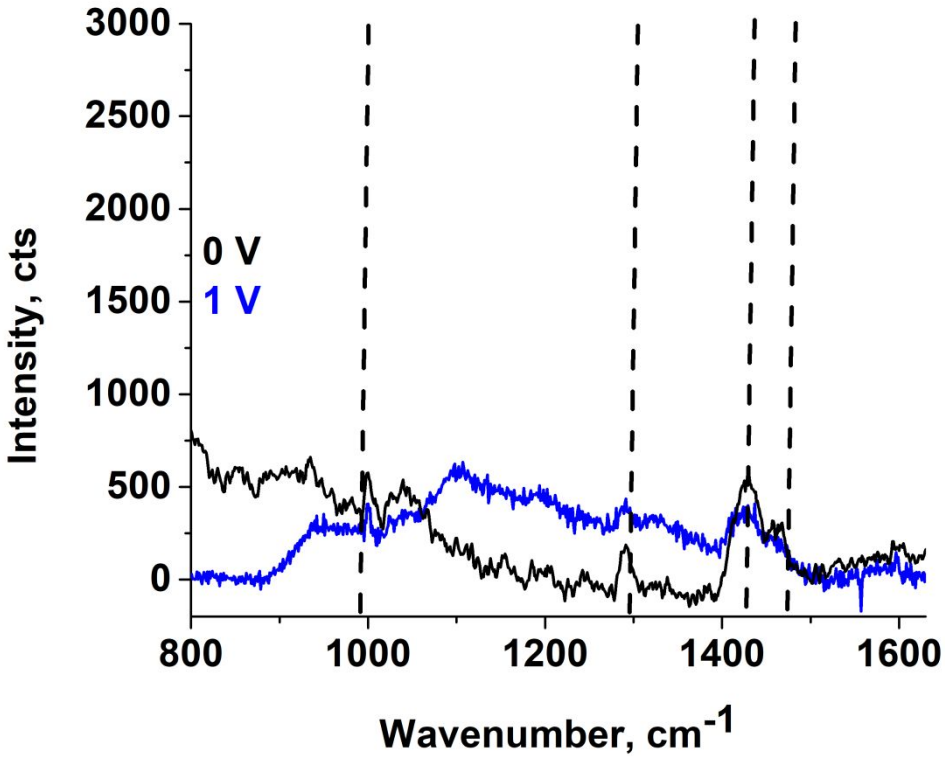

Fig. S11. Raman spectrum of BIPY-$CoCl_2$ at 0 V (black) and a potential of 1 V (blue) after excitation at 633 nm. Peaks at ~1300 cm^{-1} and ~1240^{-1} correspond to in-plane ring modes.[19,20] Peaks at ~1450 cm^{-1} correspond to CH deformation modes.[19,20] Peak at ~990 cm^{-1} corresponds to a ring-breathing mode.[19,20]

References

(1) Park, J.; Belding, L.; Yuan, L.; Mousavi, M. P. S.; Root, S. E.; Yoon, H. J.; Whitesides, G. M. Rectification in Molecular Tunneling Junctions Based on Alkanethiolates with Bipyridine-Metal Complexes. *J. Am. Chem. Soc.* **2021**, *143*, 2156–2163. https://doi.org/10.1021/jacs.0c12641.

(2) Weiss, E. A.; Kaufman, G. K.; Kriebel, J. K.; Li, Z.; Schalek, R.; Whitesides, G. M. Si/SiO2-Templated Formation of Ultraflat Metal Surfaces on Glass, Polymer, and Solder Supports: Their Use as Substrates for Self-Assembled Monolayers. *Langmuir* **2007**, *23*, 9686–9694. https://doi.org/10.1021/la701919r.

(3) Weiss, E. A.; Chiechi, R. C.; Kaufman, G. K.; Kriebel, J. K.; Li, Z.; Duati, M.; Rampi, M. A.; Whitesides, G. M. Influence of Defects on the Electrical Characteristics of Mercury-Drop Junctions: Self-Assembled Monolayers of n-Alkanethiolates on Rough and Smooth Silver. *J. Am. Chem. Soc.* **2007**, *129*, 4336.

(4) Chiechi, R. C.; Weiss, E. A.; Dickey, M. D.; Whitesides, G. M. Eutectic Gallium-Indium (EGaIn): A Moldable Liquid Metal for Electrical Characterization of Self-Assembled Monolayers. *Angew. Chemie - Int. Ed.* **2008**, *47*, 142–144. https://doi.org/10.1002/anie.200703642.

(5) Yoon, H. J.; Liao, K. C.; Lockett, M. R.; Kwok, S. W.; Baghbanzadeh, M.; Whitesides, G. M. Rectification in Tunneling Junctions: 2,2'-Bipyridyl-Terminated n -Alkanethiolates. *J. Am. Chem. Soc.* **2014**, *136*, 17155–17162. https://doi.org/10.1021/ja509110a.

(6) Murali, M.; Palaniandavar, M. Mixed-Ligand Copper(II) Complexes with Positive Redox Potentials. *Transit. Met. Chem.* **1996**, *21*, 142–148. https://doi.org/10.1007/BF00136544.

(7) Kaes, C.; Katz, A.; Hosseini, M. W. Bipyridine: The Most Widely Used Ligand. A Review of Molecules Comprising at Least Two 2,2′-Bipyridine Units. *Chem. Rev.* **2000**, *100*, 3553–3590. https://doi.org/10.1021/cr990376z.

(8) Angel, N. R.; Khatib, R. M.; Jenkins, J.; Smith, M.; Rubalcava, J. M.; Le, B. K.; Lussier, D.; Chen, Z. (Georgia); Tham, F. S.; Wilson, E. H.; Eichler, J. F. Copper (II) Complexes Possessing Alkyl-Substituted Polypyridyl Ligands: Structural Characterization and in Vitro Antitumor Activity. *J. Inorg. Biochem.* **2017**, *166*, 12–25. https://doi.org/10.1016/j.jinorgbio.2016.09.012.

(9) Simeone, F. C.; Yoon, H. J.; Thuo, M. M.; Barber, J. R.; Smith, B. S.; Whitesides, G. M. Defining the Value of Injection Current and Effective Electrical Contact Area for EGaIn-Based Molecular Tunneling Junctions. *J. Am. Chem. Soc.* **2013**, *135*, 18131–18144.

(10) Doniach, S.; Sunjic, M. Many-Electron Singularity in X-Ray Photoemission and X-Ray Line Spectra from Metals. *J. Phys. C Solid State Phys.* **1970**, *3*, 285.

(11) Wertheim, G. K.; Butler, M. A.; West, K. W.; Buchanan, D. N. E. Determination of the Gaussian and Lorentzian Content of Experimental Line Shapes. *Rev. Sci. Instrum.* **1974**, *45*, 1369–1371. https://doi.org/10.1063/1.1686503.

(12) Shirley, D. A. High-Resolution X-Ray Photoemission Spectrum of the Valence Bands of Gold. *Phys. Rev. B* **1972**, *5*, 4709.

(13) Olivero, J. J.; Longbothum, R. L. Empirical Fits to the Voigt Line Width. *J. Quant. Spectrosc. Radiat. Transf.* **1977**, *17*, 233–236.

(14) Jablonski, A.; Powell, C. J. Formalism and Parameters for Quantitative Surface Analysis by Auger Electron Spectroscopy and X-ray Photoelectron Spectroscopy. *Surf. Interface Anal.* **1993**, *20*, 771–786. https://doi.org/10.1002/sia.740200906.

(15) Powell, C. J.; Jablonski, A. Electron Effective Attenuation Lengths for Applications in Auger Electron Spectroscopy and X-Ray Photoelectron Spectroscopy. *Surf. Interface Anal.* **2002**, *33*, 211–229. https://doi.org/10.1002/sia.1204.

(16) Byeon, S. E.; Kim, M.; Yoon, H. J. Maskless Arbitrary Writing of Molecular Tunnel Junctions. *ACS Appl. Mater. Interfaces* **2017**, 40556–40563. https://doi.org/10.1021/acsami.7b14347.

(17) Valiev, M.; Bylaska, E. J.; Govind, N.; Kowalski, K.; Straatsma, T. P.; Van Dam, H. J. J.; Wang, D.; Nieplocha, J.; Apra, E.; Windus, T. L.; de Jong, W. A. NWChem: A Comprehensive and

Scalable Open-Source Solution for Large Scale Molecular Simulations. *Comput. Phys. Commun.* **2010**, *181*, 1477–1489. https://doi.org/http://dx.doi.org/10.1016/j.cpc.2010.04.018.

(18) Hanwell, M. D.; Curtis, D. E.; Lonie, D. C.; Vandermeersch, T.; Zurek, E.; Hutchison, G. R. Avogadro: An Advanced Semantic Chemical Editor, Visualization, and Analysis Platform. *J. Cheminform.* **2012**, *4*, 17. https://doi.org/10.1186/1758-2946-4-17.

(19) Yan, X.; Li, P.; Yang, L.; Liu, J. Time-Dependent SERS Spectra Monitoring the Dynamic Adsorption Behavior of Bipyridine Isomerides Combined with Bianalyte Method. *Analyst* **2016**, *141*, 5189–5194. https://doi.org/10.1039/C6AN00771F.

(20) Moissette, A.; Batonneau, Y.; Brémard, C. Conformation and Protonation of 2,2‘-Bipyridine and 4,4‘-Bipyridine in Acidic Aqueous Media and Acidic ZSM-5 Zeolites: A Raman Scattering Study. *J. Am. Chem. Soc.* **2001**, *123*, 12325–12334. https://doi.org/10.1021/ja011787b.